Enhancement of the Intermolecular Magnetic Exchange through Halogen···Halogen interactions in Bisadeninium Rhenium(IV) Salts

Enhancement of the Intermolecular Magnetic Exchange through Halogen···Halogen interactions in Bisadeninium Rhenium(IV) Salts

Donatella Armentano,[a] Miguel A. Barquero,[b] Carlos Rojas-Dotti,[b] Nicolas Moliner,[b] Giovanni De Munno,[a] Euan K. Brechin*[c] and José Martínez-Lillo*[b]

[a]Dipartimento di Chimica e Tecnologie Chimiche (CTC), Università della Calabria, via P. Bucci 14/c, 87036, Rende, Cosenza, Italy
[b]Instituto de Ciencia Molecular (ICMol), Universitat de València, c/ Catedrático José Beltrán 2, 46980, Paterna, Valencia, Spain
[c]EaStCHEM School of Chemistry, The University of Edinburgh, David Brewster Road, EH9 3FJ, Edinburgh, UK

ABSTRACT: Two novel Re^{IV} salts of general formula $[H_2ade]_2[Re^{IV}X_6]X_2{\cdot}4H_2O$ [H_2ade^{2+} = 9H-adenine-1,7-diium; X = Cl(**1**) and Br(**2**)] have been synthesized and magneto-structurally characterized. **1** and **2** are isostructural salts that crystallize in the orthorhombic system with space group *Fdd*2. Both compounds are made up of discrete mononuclear $[Re^{IV}X_6]^{2-}$ and X^- anions and doubly protonated adenine cations. The six-coordinate rhenium(IV) ion is bonded to six halide ligands [X = Cl (**1**) and Br (**2**)] in an octahedral geometry. Short intermolecular Re^{IV}–X···X–Re^{IV} interactions, as well as Re^{IV}–X···H–N(H_2ade) and Re^{IV}–X···H–O_w hydrogen bonds, are present in the crystal lattice of **1** and **2**. Magnetic susceptibility measurements on polycrystalline samples of **1** and **2** in the temperature range 2.0-300 K show the occurrence of significant intermolecular antiferromagnetic interactions in both compounds, resulting in the observation of maxima in χ_M at *ca*. 6.0 (**1**) and 12.0 K (**2**). The larger spin delocalization from the Re^{IV} ion onto their peripheral bromide ligands when compared to the chloride ligands accounts for the enhancement of the magnetic exchange observed in **2**.

Adenine is one of the five main natural nucleobases that are precursors and part of the self-assembled structures of the nucleic acids (DNA and RNA). As with other nucleobases, adenine has been studied for decades due to its capacity to establish diverse noncovalent interactions and its potential metal ion binding ability in complex, natural and artificial nanostructures.[1-11] It is well-known that the combination of hydrogen bonds and π-π stacking interactions among nucleobases provides the conformation and function of macromolecular biological systems.[1-3] Protonated and deprotonated nucleobases play a key role in many biochemical processes, and can also generate supramolecular compounds of interest in crystal engineering, molecular recognition, liquid crystals, molecule-based magnetism and materials science.[12-19]

The nucleobase adenine presents up to four endocyclic (N1, N3, N7 and N9) and one exocyclic (N6) protonatable N-atoms (in basicity order: N9 > N1 > N7 > N3 > N6) which can afford a wide range of neutral tautomers and protonated forms (Chart 1). Both organic and inorganic salts based on mono- and diprotonated adenine [adeninium (B) or bisadeninium (C), respectively] are found in the literature. While there exist paramagnetic compounds with adeninium, all bisadeninium-based salts reported to date are diamagnetic in nature.[20-26]

Chart 1. Molecular Structures of 9H-adenine (A) and its mono- and diprotonated, 9H-adenine-1-ium (B) and 9H-adenine-1,7-diium (C) Derivatives

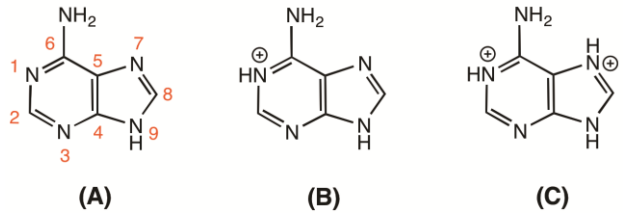

Anionic halorhenate(IV) salts are very appealing because of their unique magnetic properties, which include both slow relaxation and quantum tunneling of the magnetization and long-range magnetic order originating from single-ion or cooperative magnetic behaviours, respectively.[27-46] In particular, the simple hexahalorhenate(IV) salts $[Re^{IV}X_6]^{2-}$ (X = F, Cl, Br, and I) of paramagnetic and diamagnetic cations generally show significant short-range intermolecular ferro- or antiferromagnetic interactions, which are mainly transmitted through relatively short intermolecular Re–X···X–Re contacts, occasionally leading to collective magnetic phenomena such as ferromagnetism and spin canting (weak ferromagnetism).[47-59]

Herein we report the synthesis and magneto-structural characterization of two novel Re^{IV} compounds of general formula $[H_2ade]_2[Re^{IV}X_6]X_2{\cdot}4H_2O$ [H_2ade^{2+} = 9H-adenine-1,7-diium; X = Cl (**1**) and Br (**2**)]. **1** and **2** are the first paramagnetic salts based on diprotonated adenine.

Results and Discussion

Structure Description of 1 and 2

Compounds **1** and **2** are isostructural salts that crystallize in the orthorhombic system with space group *Fdd*2 (Table 1). Both compounds are made up of discrete mononuclear $[Re^{IV}X_6]^{2-}$ and X^- anions [X = Cl (**1**) and Br (**2**)], bisadeninium cations, and water molecules of crystallization, which self-assemble in the crystal lattice through an intricate and extended network of hydrogen bonds and X···X type intermolecular interactions (Figures 1-5 and Figures S1-S5).

The asymmetric unit in **1** and **2** consists of half a $[Re^{IV}X_6]^{2-}$ anion, with the rhenium atom lying on a special position, a chloride (**1**) or bromide (**2**) ion, a bisadeninium molecule, together with two crystallization water molecules. Figure 1 shows the $[Re^{IV}Br_6]^{2-}$ anion with its second-sphere coordination environment for **2** (see Figure S1 for **1**).

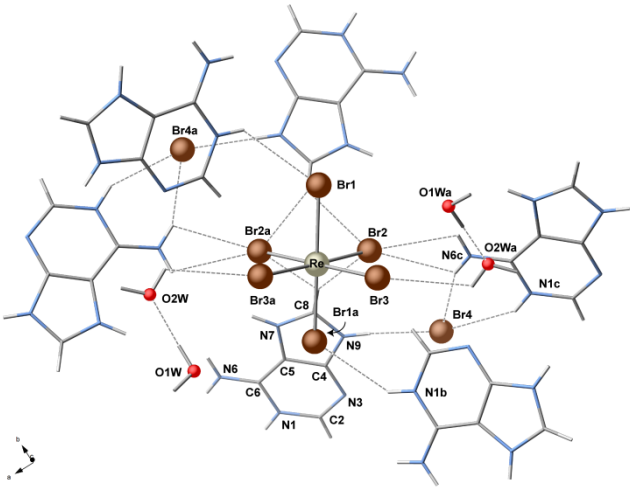

Figure 1. Molecular structure of the $[ReBr_6]^{2-}$ anion in **2** with atom numbering scheme, showing the closest supramolecular interactions with the $[H_2ade]^{2+}$ cations and Br^- anions. Hydrogen bonds are depicted as dashed lines. Color code: Re, pale gray; Br, brown; O, red; N, blue; C, dark gray; H, white. [Symmetry code: (a) = -¾ - *x*, 1/2 - *y*, *z*; (b) = *x*-1/4, ¾ - *y*, *z* -¾].

Each six-coordinate Re^{IV} ion in **1** and **2** is bonded to six chloride (**1**) or bromide (**2**) ions in a slightly distorted octahedral environment. The Re–Cl and Re-Br bond lengths [average values of the Re-Cl and Re-Br distances of 2.359(1) and 2.508(5) Å, respectively] are in agreement with those found in previously reported Re^{IV} halide complexes.[47-60] The doubly protonated adenine cation is planar, as expected (see Figures 1-4 and S1-S4 for **2** and **1**, respectively).

Table 1. Summary of the Crystal Data and Structure Refinement Parameters for 1 and 2

Compound	**1**	**2**
Formula	$C_{10}H_{22}Cl_8N_{10}O_4Re$	$C_{10}H_{22}Br_8N_{10}O_4Re$
M_r/g mol^{-1}	816.17	1171.85
Crystal system	orthorhombic	orthorhombic
Space group	*Fdd*2	*Fdd*2
a/Å	17.9892(4)	18.6623(5)
b/Å	39.2724(8)	39.9223(11)
c/Å	7.13685(16)	7.35595(18)
α/°	90	90
β/°	90	90
γ/°	90	90
V / Å^3	5042.04(19)	5480.4(2)
Z	8	8
D_c/g cm^{-3}	2.150	2.841
μ(Mo-K$_\alpha$)/mm^{-1}	5.709	16.138
F(000)	3160	4312
T/*K*	170	120
Goodness-of-fit on F^2	1.038	1.085
R_1 [$I > 2\sigma(I)$]	0.0238	0.0208
wR_2 [all data]	0.0468	0.0333
$\Delta\rho_{max,\ min}$/e Å^{-3}	1.120 and -1.500	0.968 and -0.796

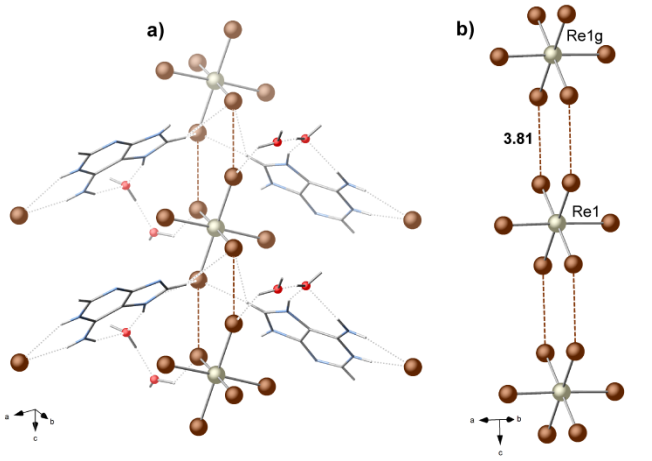

Figure 2. a) View of a fragment of the supramolecular motif generated by hydrogen bonds involving $[H_2ade]^{2+}$ cations, Br^- and $[Re^{IV}Br_6]^{2-}$ anions and lattice water molecules in the crystal packing of **2**. b) Perspective view of the branched chain connecting $[Re^{IV}Br_6]^{2-}$ anions through intermolecular

double Br···Br type interactions (dashed brown lines) and growing in the *c*-axis direction.

The average values of the C–C and C–N bond lengths are in agreement with those found in their corresponding salts.[20-26,61]

As expected, the additional protonation at the N1 and N7 nitrogen atoms makes the bisadeninium cations behave as excellent H-bond donors in **1** (Figures S2 and S4) and **2** (Figures 2 and 4). In fact, they are involved in three types of hydrogen bonds with the $[Re^{IV}X_6]^{2-}$ or X^- anions [X = Cl (**1**) and Br (**2**)], and the lattice water molecules acting as H-bond acceptors (see Figures 3 and S3).

Nitrogen atoms N1, N6 and N9 interact with co-crystallized X^- anions through N-H···X hydrogen bonds [N1···Cl4, N6···Cl4 and N9···Cl4c distances of 3.246(4), 3.197(4) and 3.084(4) Å in **1**, with N1···Br4, N6···Br4 3.332(4) and N9···Br4c distances of 3.470(4), 3.332(4) and 3.237(4) Å in **2**, (c) = x-1/2, y, z-1/2]. N1 and N6 are connected to the $[Re^{IV}X_6]^{2-}$ anions through bifurcated three-centered N-H···X hydrogen bonds [Figures S3 and 3; N1···Cl1d and N6···Cl2e distances of 3.445(4) and 3.093(4) Å in **1**, with N1···Br1d and N6···Br2e distances of 3.539(4) and 3.202(1) in **2**, (d) = -x+7/4, y+1/4, z+3/4; (e) = -x+3/2, -y+1/2, z] (Tables 2-3). The third type of N-H···O hydrogen bonds involves bisadeninium cations and water molecules linked to N6 and N7 [N6···O1w and N7···O1w distances being 2.975(6) and 2.751(6) Å in **1** and 2.965(6) and 2.773(5) in **2**].

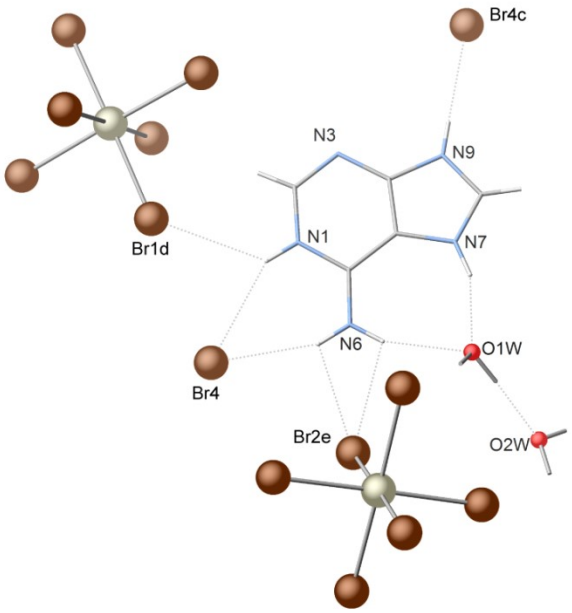

Figure 3. Perspective view of a fragment of crystal packing in **2** showing detailed N-H···Br and N-H···O_{water} hydrogen bonds interactions (dashed lines), which involve the diprotonated $[H_2ade]^{2+}$ cation.

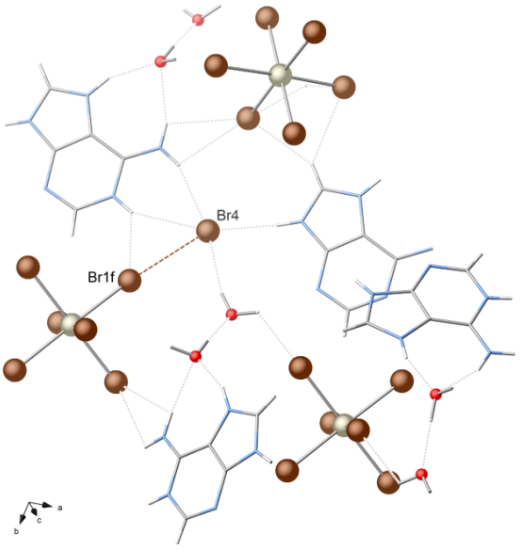

Figure 4. Details of the X···$[Re^{IV}X_6]^{2-}$ interaction (dashed brown lines) and surroundings built through H-bonds (dashed gray lines) involving the X^- anion in the crystal packing of **2.**

This supramolecular $[H_2ade]$···$[H_2O]$ aggregate is further linked to another water molecules generating "water dimers" acting as linkers towards free X^- and $[Re^{IV}X_6]^{2-}$ anions [$O1_W$···$O2_W$ 2.746(6) and 2.789(5) Å] (Figures 4 and S4). The resulting supramolecular assembly defines a *pseudo-butterfly* motif (Figures 2a and S2a).

Looking at the crystal packing of **1** and **2**, it is evident that an additional supramolecular interaction exits between X^- anions of either neighboring $[Re^{IV}X_6]^{2-}$ complexes (Figures 2 and S2) or the free X^- anions (Figures 4 and S4), associated with the presence of relatively short X···X distances [Cl4···Cl1f and Cl2···Cl3g distances of 3.58 and 3.80 Å for **1**, and Br4···Br1f and Br2···Br3g distances of 3.63 and 3.81 Å for **2**, (f) = ½+x, 1+y, ¾ +z; (g) = x, y, 1-z].[60] One of these intermolecular halogen bonding interactions in **1** and **2** lead to branched chains of $[Re^{IV}X_6]^{2-}$ anions with appended X^- residues, growing in the *c*-axis direction (Figures 2 and S2). The intrachain Re1···Re1g distances through the double Re^{IV}–X···X–Re^{IV} bridges are 7.137(1) (**1**) (Figure S2) and 7.356(1) Å (**2**) (Figure 2), while the shortest interchain Re1···Re1h separations being 9.677(1) and 10.030(1) Å in **1** and **2**, respectively [(h) = ½+x, y, ½+z].

Finally, weak C-H···X type interactions between $[H_2ade]^{2+}$ cations and $[Re^{IV}X_6]^{2-}$ anions support the cohesion of the whole supramolecular network in the crystal structures of **1** and **2** [C···X distances varying in the ranges of 3.379(5)-3.832(5) Å and 3.521(5)-3.924(5) Å for **1** (Figure S4) and **2** (Figure 4)].

Overall, the supramolecular packing of **1** and **2** is best described as alternating sheets of bisadeninium cations and $[Re^{IV}X_6]^{2-}$ anions developing along the *b* axis (Figure 5 and S5). The halide ions are grasped between the nucleobase entities through hydrogen bonds with the nitrogen atoms and lattice water molecules (Figures 3 and 4). Layers of bisadeninium cations and hexahalorhenate(IV) anions further interact by anion–cation, cation–water and water–water hydrogen bonds (Figure 3). This supramolecular network is further supported by halogen bonding interactions (see Figures 2 and 4 for **2** and Figures S2 and S4 for **1**).

Table 2. Hydrogen-Bonding Interactions in 1[a]

D-H···A	D-H/Å	H···A/Å	D···A/Å	(DHA)/°
N(1)-H(1)···Cl(1d)	0.860	2.87	3.445(4)	125.8
N(1)-H(1)···Cl(4)	0.860	2.47	3.246(4)	149.9
N(6)-H(6A)···Cl(4)	0.860	2.41	3.197(4)	152.8
N(9)-H(9)···Cl(4c)	0.89(6)	2.21(6)	3.084 (4)	168(7)
N(6)-H(6B))···O(1w)	0.86(5)	2.15	2.965(6)	158.3
N(7)-H(7)···O(1w)	0.78(5)	1.99(5)	2.751(6)	163(5)
O(1w)-H(2w)···O(2w)	0.93(4)	1.82(4)	2.746(6)	172(5)
O(2w)-H(4w)···Cl(4h)	0.97(3)	2.33(4)	3.292(4)	170(6)

[a]Symmetry codes: (c) = x-1/2, y, z-1/2; (d) = -x+7/4, y+1/4, z+3/4; (h) = -x+9/4, y-1/4, z-1/4.

Table 3. Hydrogen-Bonding Interactions in 2[a]

D-H···A	D-H/Å	H···A/Å	D···A/Å	(DHA)/°
N(1)-H(1)···Br(1d)	0.860	2.92	3.539(4)	130.0
N(1)-H(1)···Br(4)	0.860	2.70	3.470(4)	149.2
N(6)-H(6A)···Br(4)	0.860	2.52	3.332(4)	157.4
N(9)-H(9)···Br(4c)	0.85(5)	2.40(5)	3.237 (4)	170(6)
N(6)-H(6B)···O(1w)	0.86(5)	2.15(5)	2.975(6)	160.0
N(7)-H(7)···O(1w)	0.90(5)	1.91(5)	2.773(5)	158(5)
O(1w)-H(2w)···O(2w)	0.91(3)	1.88(3)	2.789(5)	175(6)
O(2w)-H(4w)···Br(4h)	0.91(3)	2.58(4)	3.474(4)	168(5)

[a]Symmetry codes: (c) = x-1/2, y, z-1/2; (d) = -x+7/4, y+1/4, z+3/4; (h) = -x+9/4, y-1/4, z-1/4.

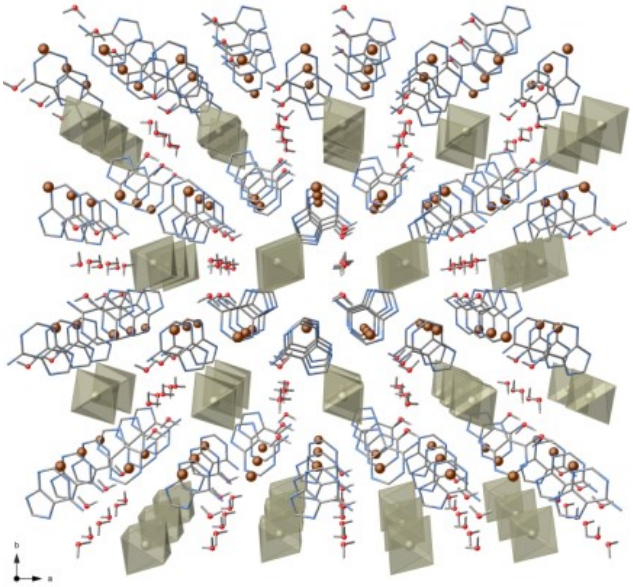

Figure 5. Perspective view along the crystallographic *c* axis of the overall supramolecular assembly of cations, anions and water molecules of **2**, showing the regularly intercalating $[H_2ade]^{2+}$ cations and the eclipsed one-dimensional arrangement of $[ReX_6]^{2-}$ anions along the *c*-axis direction through double Re^{IV}–X···X–Re^{IV} contacts.

Magnetic properties of 1 and 2

Direct current magnetic susceptibility measurements were carried out on microcrystalline samples of **1** and **2** in the 2.0-300 K temperature range, under external magnetic fields of 0.1 T (at $T > 30$ K) and 0.025 T (at $T < 30$ K). The magnetic properties of **1** and **2** in the form of both $\chi_M T$ and χ_M *vs*. *T* plots (χ_M being the molar magnetic susceptibility) are shown in Figures 6 and 7, respectively. At room temperature, the $\chi_M T$ value is 1.53 $cm^3\ mol^{-1}\ K$ for **1** and **2**, a value which is very close to that expected for a magnetically isolated Re^{IV} ion ($S_{Re} = 3/2$) with $g = 1.8–1.9$.[27] Upon cooling, the $\chi_M T$ values for **1** and **2** continuously decrease reaching values of 0.10 (**1**) and 0.05 $cm^3\ mol^{-1}\ K$ (**2**) at 2.0 K. The decrease of $\chi_M T$ observed for **1** and **2** is likely due to the presence of intermolecular interactions and/or zero-field splitting (zfs) effects.[27-46] The presence of a maximum in the magnetic susceptibility at *ca*. 6.0 (**1**) and 12.0 K (**2**) (see insets of Figs. 6 and 7) unambiguously supports the occurrence of antiferromagnetic exchange interactions between the Re^{IV} ions. No out-of-phase signals in the ac magnetic susceptibility are observed for either **1** or **2**.

In fact, a detailed inspection of the crystal packing features of **1** and **2** reveals the presence of short X···X contacts between the paramagnetic $[ReX_6]^{2-}$ anions (Figs. 2 and S2), which could serve as convenient pathways for the transmission of the exchange interactions between the magnetically anisotropic Re^{IV} ions.[27,47-59]

In order to analyze the magnetic behavior of **1** and **2**, we have employed the spin Hamiltonian for a mononuclear rhenium(IV) complex of eq (1),[62] where D is the zero-field splitting parameter and $g_{\parallel}$ and $g_{\perp}$ are the parallel and perpendicular components of the Landé factor of an axially distorted Re^{IV} ion.

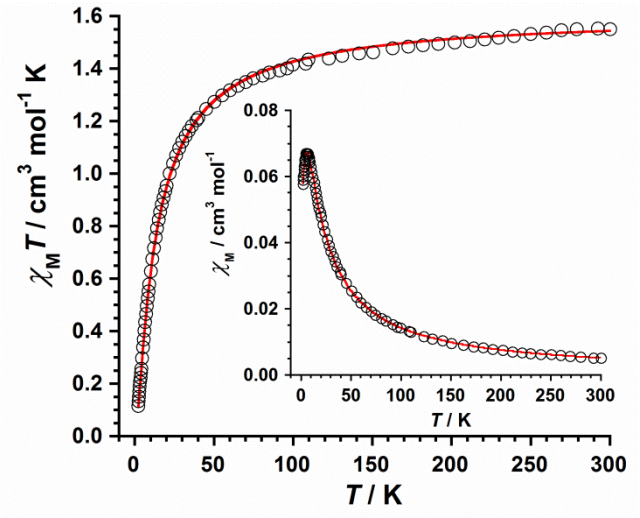

Figure 6. Thermal variation of the $\chi_M T$ product for **1**. The solid red line represents the best-fit of the experimental data (see text). The inset shows the temperature dependence of the magnetic susceptibility.

$$\hat{H} = D\left[(\hat{S}_Z)^2 - S(S+1)/3\right] + g_{//}\beta H_Z \hat{S}_Z + g_{\perp}\beta\,(H_X \hat{S}_X + H_Y \hat{S}_Y) \quad (1)$$

The first term in eq (1) corresponds to the zero-field splitting ($2D$ being the energy gap between the two $M_S = \pm 3/2$ and $M_S = \pm 1/2$ Kramers doublet), and the last two terms the Zeeman effects.

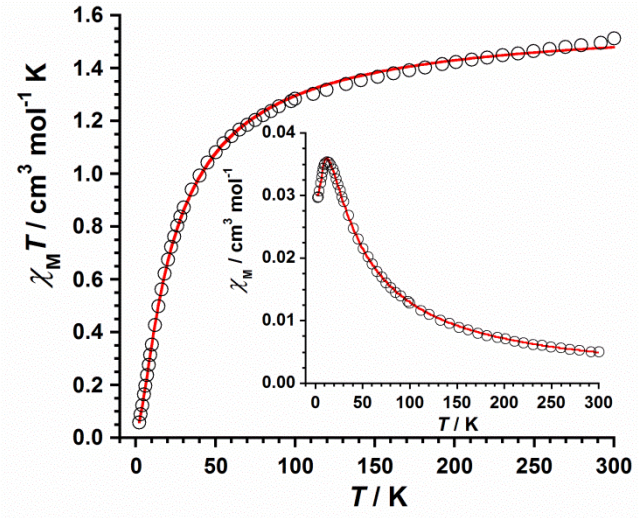

Figure 7. Thermal variation of the $\chi_M T$ product for **2**. The solid red line represents the best-fit of the experimental data (see text). The inset shows the temperature dependence of the magnetic susceptibility.

The magnetic susceptibility data of **1** and **2** were fitted through the appropriate theoretical expression derived from eq (1) by including an additional θ term to account for the intermolecular magnetic interactions (zj), where θ is the Weiss factor defined as $\theta = zjS_{Re}(S_{Re} + 1)/3k_B$ within the mean field approximation.[62] Attempts to fit the experimental data of **1** and **2** through a Heisenberg linear chain coupling model gave low-quality fits, especially in the low temperature region. The least-squares fits of the experimental data for the isotropic case ($g_{//} = g_{\perp} = g$) gave $|D|$ = 8.03 cm^{-1}, g = 1.85 and θ = –12.6 K with R = 8.7 x 10^{-5} for **1**, and $|D|$ = 5.86 cm^{-1}, g = 1.84 and θ = –16.7 K with R = 2.0 x 10^{-4} for **2** {R being the agreement factor defined as $\Sigma_i[(\chi_M T)_i^{obs} - (\chi_M T)_i^{calc}]^2/[(\chi_M T)_i^{obs}]^2$} (solid red lines in Figures 6 and 7). Hence, the estimated values of the intermolecular magnetic exchange parameter (zj) are –7.0 and –9.3 cm^{-1} for **1** and **2**, respectively.

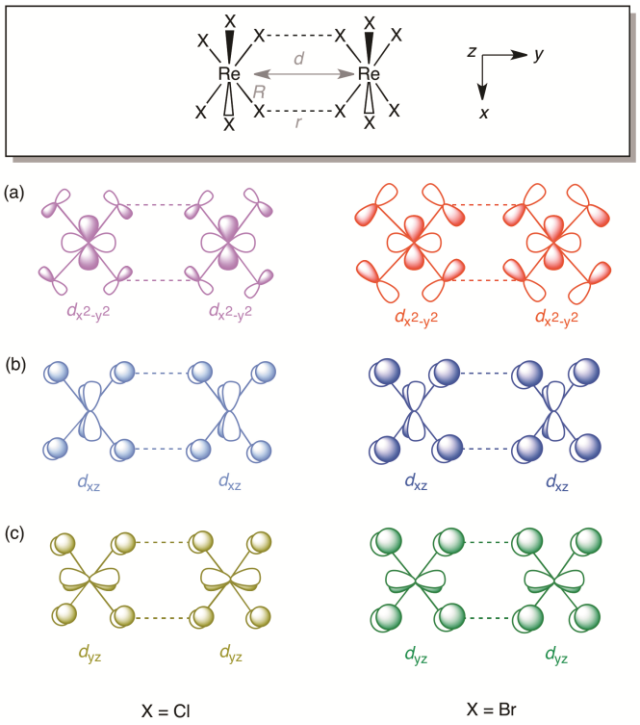

Figure 8. Schematic of the intermolecular double bridging network for **1** and **2**, {Re^{IV}–X···X–Re^{IV}}$_2$, showing the relative orientation of the $d_{x^2-y^2}/d_{x^2-y^2}$ (**a**), d_{xz}/d_{xz} (**b**), and d_{yz}/d_{yz} (**c**) pairs of magnetic orbitals of the octahedral Re^{IV} ions.

The obtained values of g and D for **1** and **2** are in agreement with those previously reported for compounds containing $[ReX_6]^{2-}$ anions.[47-59] The negative sign of the θ values obtained from the fits supports the occurrence of significant antiferromagnetic interactions between the Re^{IV} ions, the zj value of **2** being greater than that of **1**.

These results can be explained, at least in part, by the different nature of the halide ligands which are involved in the intermolecular double bridging network for **1** and **2**, $\{Re^{IV}–X\cdots X–Re^{IV}\}_2$ [X = Cl (**1**) and Br (**2**)], as illustrated in Figure 8. Given that **1** and **2** are isostructural salts and the intermolecular X···X distance is the same in both compounds [*r* = 3.80 (**1**) and 3.81 Å (**2**)], the stronger magnitude of the magnetic exchange coupling in **2** is likely due to the more diffuse character of the 4*p* orbitals of the bromide ions, compared to the 3*p* orbitals of the chloride ions in **1**, in spite of the larger Re-X bond lengths [*R* = 2.359(1) (**1**) and 2.508(5) Å (**2**)] and intermolecular Re···Re separation [d = 7.137(1) (**1**) and 7.356(1) Å (**2**)]. This feature leads to an increase in the overlap between either the σ-type $d_{x^2-y^2}/d_{x^2-y^2}$ or the π-type d_{xz}/d_{xz} and d_{yz}/d_{yz} pairs of magnetic orbitals, thus favoring the magnetic coupling between the Re^{IV} ions across the intermolecular Re-X···X-Re exchange pathways.

Conclusions

In summary, the crystal structures and magnetic properties of two novel Re^{IV} compounds, of general formula $[H_2ade]_2[ReX_6]X_2{\cdot}4H_2O$ [X = Cl(**1**) and Br(**2**)], based on $[ReX_6]^{2-}$ anions and doubly protonated adenine cations have been studied for the first time. In both compounds, the organic cations and the inorganic anions self-assemble into novel supramolecular structures through a combination of hydrogen and halogen bonds. The latter are responsible for propagating relatively strong intermolecular antiferromagnetic exchange interactions between the Re^{IV} ions through short Re-X···X-Re contacts. Given that **1** and **2** are isostructural compounds, exhibiting the same value of the shortest X···X distance, we can directly observe the effect of changing the halide ligand on the magnetic exchange. As evidenced by our results, the larger diffuse character of the 4*p* orbitals of the bromide ligands when compared to the 3*p* orbitals of chloride ligands would account for the enhancement of the magnetic exchange observed in **2**. This feature may therefore prove to be an effective tool to have in mind when attempting to increase the magnetic coupling in this type of compounds in order to obtain rhenium(IV)-based molecular magnetic materials with higher ordering temperatures.

Experimental Section

Materials and Physical Measurements

All manipulations were performed under aerobic conditions, using materials as received (reagent grade). $(NH_4)_2[ReCl_6]$ and K_2ReBr_6 were prepared following the synthetic methods described in the literature.[63]
Elemental analyses (C, H, N) were performed by the Central Service for the Support to Experimental Research (SCSIE) at the University of Valencia. Infrared spectra of **1** and **2** were recorded (as KBr pellets) with a PerkinElmer Spectrum 65 FT-IR spectrometer in the 4000-400 cm^{-1} region. Variable-temperature, solid-state direct current (dc) magnetic susceptibility data down to 2.0 K were collected on a Quantum Design MPMS-XL SQUID magnetometer equipped with a 7 T dc magnet. Experimental magnetic data were corrected for the diamagnetic contributions of the constituent atoms by using Pascal's constants.[64,65]

Preparation of Compounds 1 and 2

1. A mixture of $(NH_4)_2[ReCl_6]$ (0.10 mmol, 43.5 mg) and adenine (0.20 mmol, 27.0 mg) was dissolved in HCl (6.0 M, 15.0 mL) and heated to 60 °C with continuous stirring for 30 minutes. The resulting green solution was filtered and left to evaporate. Pale green crystals of **1** were grown in 2-3 days. Yield: 31 %. Crystals suitable for X-ray diffraction studies were obtained by reducing the amount of adenine to 1.5 equivalents. Anal. Cald. (found) for $C_{10}H_{22}N_{10}O_4Cl_8Re$ (**1**): C, 14.7 (14.5); H, 2.7 (2.9); N, 17.2 (17.6) %. IR peaks (KBr/cm^{-1}): 3554 (m), 3474 (m), 3319 (m), 3196 (m), 3119 (m), 3069 (m), 2921 (m), 2849 (m), 2591 (m), 2527 (m), 2360 (w), 1897 (m), 1705 (vs), 1624 (s), 1507 (m), 1438 (m), 1378 (s), 1292 (m), 1197 (m), 1161 (m), 1106 (w), 1022 (m), 941 (s), 892 (m), 812 (m), 774 (m), 718 (m), 613 (m), 603 (m), 548 (m), 548 (w).

2. A mixture of K_2ReBr_6 (0.10 mmol, 74.4 mg) and adenine (0.20 mmol, 27.0 mg) was dissolved in HBr (6.0 M, 15.0 mL) and heated to 55-60 °C with continuous stirring for 30 minutes. An orange solution was obtained, filtered and left to evaporate. Orange crystals of **2** were grown in 2-3 days. Yield: 29 %. As in **1**, crystals suitable for X-ray diffraction studies were obtained by reducing the amount of adenine to 1.5 equivalents. Anal. Cald. (found) for $C_{10}H_{22}N_{10}O_4Br_8Re$ (**2**): C, 10.3 (10.5); H, 1.9 (1.9); N, 12.0 (11.8) %. IR peaks (KBr/cm^{-1}): 3579 (m), 3484 (m), 3310 (m), 3190 (m), 3109 (m), 3063 (m), 2915 (m), 2842 (m), 2591 (m), 2525 (m), 2344 (w), 1882 (m), 1701 (vs), 1621 (s), 1504 (m), 1434 (m), 1376 (s), 1288 (m), 1193 (m), 1153 (m), 1020 (m), 940 (m), 893 (m), 825 (m), 771 (m), 717 (m), 612 (m), 600 (m), 546 (w), 474 (w).

X-ray Data Collection and Structure Refinement

X-ray diffraction data on single crystals of dimensions 0.72 x 0.11 x 0.08 (**1**) and 0.46 x 0.12 x 0.09 mm^3 (**2**) were collected on Rigaku Oxford Diffraction XCalibur (**1**) and Rigaku Oxford Diffraction SuperNova (**2**) X-ray diffractometers using Mo-K_α radiation (λ = 0.71073 Å). CrysAlisPro was used for diffractometer control and data processing. Crystal parameters and refinement results for **1** and **2** are summarized in Table 1. The structures of **1** and **2** were solved by direct methods and subsequently completed by Fourier recycling using version 2013/4 of SHELXL.[66-68] The final full-matrix least-squares refinements on F^2, minimizing the function $\sum w(|F_o|-|F_c|)^2$,

reached convergence with the values of the discrepancy indices given in Table 1. All non-hydrogen atoms were refined anisotropically. H7 and H9 atoms of the 9H-adenine-1,7-diium cation were found from the ΔF map and refined, whereas the rest of hydrogen atoms were set in calculated positions and refined using a riding model. The graphical manipulations were performed with CrystalMaker Software.[69] CCDC 1556332 (**1**) and 1556333 (**2**).

ASSOCIATED CONTENT

Supporting Information. X-ray crystallographic data in CIF format for compounds **1** and **2**. Figures S1-S5. This material is available free of charge via the Internet at http://pubs.acs.org. Data is available from Edinburgh Datashare: http://datashare.is.ed.ac.uk.

AUTHOR INFORMATION

Corresponding Author

*E-mail: ebrechin@ed.ac.uk. Tel: +44 (0)131 650 7545 (E.K.B.)
*E-mail: lillo@uv.es. Tel: +34 963544460 (J.M.-L.)

Notes

The authors declare no competing financial interest.

ACKNOWLEDGMENTS

Financial support from the Italian Ministero dell'Istruzione, dell'Università e della Ricerca Scientifica (MIUR), the Spanish Ministry of Economy and Competitiveness (MINECO) with projects CTQ2016-75068-P and MDM-2015-0538 (Excellence Unit *María de Maeztu*) is gratefully acknowledged. EKB thanks the EPSRC. JML thanks the Spanish MINECO for a *Ramón y Cajal* researcher contract. We gratefully acknowledge Dr. Gary Nichol for single-crystal X-ray diffraction data collections and Dr. Rafael Ruiz-García for helpful discussions.

REFERENCES

(1) Lippert, B. *Coord. Chem. Rev*. **2000**, *200–202*, 487–516.
(2) Beobide, B.; Castillo, O.; Cepeda, J.; Luque, A.; Pérez-Yáñez, S.; Román, P.; Thomas-Gipson, J. *Coord. Chem. Rev*. **2013**, *257*, 2716–2736.
(3) Lippert, B.; Sanz Miguel, P. J. *Acc. Chem. Res*. **2016**, *49*, 1537-1545.
(4) Stolar, T.; Lukin, S.; Požar, J.; Rubčić, M.; Day, G. M.; Biljan, I.; Jung, D. S.; Horvat, G.; Užarević, K.; Meštrović, E.; Halasz, I. *Cryst. Growth Des*. **2016**, *16*, 3262–3270.
(5) Geday, A.; De Munno, G.; Medaglia, M.; Anastassopoulou, J.; Theophanides, T. *Angew. Chem., Int. Ed. Engl.* **1997**, *36*, 511-513.
(6) De Munno, G.; Medaglia, M.; Armentano, D.; Anastassopoulou, J.; Theophanides, T. *J. Chem. Soc., Dalton Trans*. **2000**, 1625-1629.
(7) García-Terán, J. P.; Castillo, O.; Luque, A.; García-Couceiro, U.; Román, P.; Lezama, L. *Inorg. Chem*. **2004**, *43*, 4549–4551.
(8) Mastropietro, T. F.; Armentano, D.; Marino, N.; De Munno, G.; Anastassopoulou, J.; Theophanides, T. *Cryst. Growth Des*. **2007**, *7*, 609–612.
(9) Mastropietro, T. F.; Armentano, D.; Grisolia, E.; Zanchini, C.; Julve, M.; Lloret F.; De Munno, G. *Dalton Trans*. **2008**, 514–520.
(10) Marino, N.; Armentano, D.; De Munno, G. *Inorg. Chim. Acta* **2016**, *452*, 229–237.
(11) Thomas-Gipson, J.; Beobide, G.; Castillo, O.; Luque, A.; Pérez-Yáñez, S.; Román, P. *Eur. J. Inorg. Chem*. **2017**, 1333–1340.
(12) Thomas-Gipson, J.; Beobide, G.; Castillo, O.; Cepeda, J.; Luque, A.; Pérez-Yáñez, S.; Aguayo, A. T.; Román, P. *CrystEngComm* **2011**, *13*, 3301-3305.
(13) Thomas-Gipson, J.; Beobide, G.; Castillo, O.; Fröba, M.; Hoffmann, F.; Luque, A.; Pérez-Yáñez, S.; Román, P. *Cryst. Growth Des*. **2014**, *14*, 4019–4029.
(14) Thomas-Gipson, J.; Pérez-Aguirre, R.; Beobide, G.; Castillo, O.; Luque, A.; Pérez-Yáñez, S.; Román, P. *Cryst. Growth Des*. **2015**, *15*, 975–983.
(15) Nugent, P. S.; Rhodus, V. L.; Pham, T.; Forrest, K.; Wojtas, L.; Space, B.; Zaworotko, M. J. *J. Am. Chem. Soc*. **2013**, *135*, 10950-10953.
(16) Pérez-Aguirre, R.; Garikoitz, B.; Castillo, O.; de Pedro, I.; Luque, A.; Pérez-Yáñez, S.; Rodríguez-Fernández, J.; Román, P. *Inorg. Chem*. **2016**, *55*, 7755–7763
(17) Stylianou, K. C.; Warren, J. E.; Chong, S. Y.; Rabone, J.; Bacsa, J.; Bradshaw, D.; Rosseinsky, M. J. *Chem. Commun*. **2011**, 47, 3389-3391.
(18) Sivakova, S; Rowan, S. J. *Chem. Soc. Rev*. **2005**, *34*, 3213-3238.
(19) Maia Jr., F. F.; Freire, V. N.; Caetano, E. W. S.; Azevedo, D. L.; Sales, F. A. M.; Albuquerque, E. L. *J. Chem. Phys*. **2011**, *134*, 175101-175109.
(20) Hardgrove Jr., G.L.; Einstein, J. R.; Hingerty, B. E.; Wei, C. H. *Acta Cryst*. **1983**, *C39*, 88-90.
(21) Bendjeddou, L.; A.Cherouana, A.; Dahaoui, S.; Benali-Cherif, N.; Lecomte, C. *Acta Cryst*. **2003**, *E59*, 0649-0651.
(22) Bouacida, S.; Hocine, M.; Beghidja, A.; Beghidja, C. *Acta Cryst*. **2005**, *E61*, m1153-m1155.
(23) Sridhar, B.; Ravikumar, K.; Varghese, B. *Acta Cryst*. **2009**, *C65*, 0202–0206.
(24) Xiong, Z.-Q.; Ai, Y.-L.; Wen, H.-L. *Acta Cryst*. **2010**, *E66*, 0318.
(25) Guenifa, F.; Bendjeddou, L.; Cherouana, A.; Dahaoui, S.; Lecomte, C. *Acta Cryst*. **2012**, *E68*, 03266–03267.
(26) Mineki, H.; Hanasaki, T.; Matsumoto, A.; Kawasaki, T.; Soai, K. *Chem. Commun*. **2012**, *48*, 10538–10540.
(27) Martínez-Lillo, J.; Faus, J.; Lloret, F.; Julve, M. *Coord. Chem. Rev.* **2015**, *289–290*, 215–237.
(28) Ferrando-Soria, J.; Vallejo, J.; Castellano, M.; Martínez-Lillo, J.; Pardo, E.; Cano, J.; Castro, I.; Lloret, F.; Ruiz-García, R.; Julve, M. *Coord. Chem. Rev.* **2017**, *339*, 17–103.
(29) Martínez-Lillo, J.; Armentano, D.; De Munno, G.; Wernsdorfer, W.; Julve, M.; Lloret, F.; Faus, J. *J. Am. Chem. Soc*. **2006**, *128*, 14218-14219.
(30) Martínez-Lillo, J.; Armentano, D.; De Munno, G.; Wernsdorfer, W.; Clemente-Juan, J. M.; Krzystek, J.; Lloret, F.; Julve, M.; Faus, J. *Inorg. Chem*. **2009**, *48*, 3027-3038.
(31) Chiozzone, R.; González, R.; Kremer, C.; De Munno, G.; Cano, J.; Lloret, F.; Julve, M.; Faus, J. *Inorg. Chem*. **1999**, *38*, 4745-4752.
(32) Cuevas, A.; Chiozzone, R.; Kremer, C.; Suescun, L.; Mombrú, A.; Armentano, D.; De Munno, G.; Lloret, F.; Cano, J.; Faus, J. *Inorg. Chem*. **2004**, *43*, 7823-7831.

(33) Martínez-Lillo, J.; Mastropietro, T. F.; LHotel, E.; Paulsen, C.; Cano, J.; De Munno, G.; Faus, J.; Lloret, F.; Julve, M.; Nellutla, S.; Krzystek, J. *J. Am. Chem. Soc*. **2013**, *135*, 13737-13748.
(34) Pedersen, K. S.; Sigrist, M.; Sørensen, M. A.; Barra, A.-L.; Weyhermüller, T.; Piligkos, S.; Thuesen, C. A.; Vinum, M. G.; Mutka, H.; Weihe, H.; Clérac, R.; Bendix, J. *Angew. Chem. Int. Ed*. **2014**, *53*, 1351 –1354.
(35) Pop, F.; Allain, M.; Auban-Senzier, P.; Martínez-Lillo, J.; Lloret, F.; Julve, M.; Canadell, E.; Avarvari, N. *Eur. J. Inorg. Chem*. **2014**, 3855–3862.
(36) Martínez-Lillo, J.; Armentano, D.; De Munno, G.; Faus, J. *Polyhedron* **2008**, *27*, 1447-1454.
(37) Arizaga, L.; González, R.; Armentano, D.; De Munno, G.; Novak, M. A.; Lloret, F.; Julve, M.; Kremer, C.; Chiozzone R. *Eur. J. Inorg. Chem*. **2016**, 1835–1845.
(38) Martínez-Lillo, J.; Cañadillas-Delgado, L.; Cano, J.; Lloret, F.; Julve, M.; Faus, J. *Chem. Commun*. **2012**, *48*, 9242–9244.
(39) Martínez-Lillo, J.; Kong, J.; Barros, W. P.; Faus, J.; Julve, M.; Brechin, E. K. *Chem. Commun*. **2014**, *50*, 5840.
(40) Feng, X; Liu, J.-L.; Harris, T. D.; Hill, S.; Long, J. R. *J. Am. Chem. Soc.* **2012**, *134*, 7521-7529.
(41) Feng, X.; Liu, J.-L.; Pedersen, K. S.; Nehrkorn, J.; Schnegg, A.; Holldack, K.; Bendix, J.; Sigrist, M.; Mutka, H.; Samohvalov, D.; Aguilà, D.; Tong, M.-L.; Long, J. R.; Clérac, R. *Chem. Commun*. **2016**, *52*, 12905-12908.
(42) Martínez-Lillo, J.; Lloret, F.; Julve, M.; Faus, J. *J. Coord. Chem*. **2009**, *62*, 92-99.
(43) Bieńko, A.; Kłak, J.; Mroziński, J.; Kruszyński, R.; Bieńko, D. C.; Boča, R. *Polyhedron* **2008**, *27*, 2464-2470.
(44) Bieńko, A.; Kruszyński, R.; Bieńko, D. *Polyhedron* **2014**, *75*, 1-8.
(45) Benmansour, S.; Coronado, E.; Giménez-Saiz, C.; Gómez-García, C. J.; Rößer, C. *Eur. J. Inorg. Chem*. **2014**, 3949-3959.
(46) Martínez-Lillo, J.; Armentano, D.; Marino, N.; Arizaga, L.; Chiozzone, R.; González, R.; Kremer, C.; Cano, J.; Faus, J. *Dalton Trans*. **2008**, 4585-4594.
(47) Reynolds, P. A.; Moubaraki, B.; Murray, K. S.; Cable, J. W.; Engelhardt, L. M.; Figgis, B. N. *J. Chem. Soc., Dalton Trans*. **1997**, 263-268.
(48) Reynolds, P. A.; Figgis, B. N.; Martin y Marero, D. *J. Chem. Soc., Dalton Trans*. **1999**, 945-950.
(49) González, R.; Chiozzone, R.; Kremer, C.; De Munno, G.; Nicolò, F.; Lloret, F.; Julve, M.; Faus, J. *Inorg. Chem*. **2003**, *42*, 2512-2518.
(50) González, R.; Chiozzone, R.; Kremer, C.; Guerra, F.; De Munno, G.; Lloret, F.; Julve, M.; Faus, J. *Inorg. Chem*. **2004**, *43*, 3013-3019.
(51) Martínez-Lillo, J.; Armentano, D.; De Munno, G.; Lloret, F.; Julve, M.; Faus, J. *Cryst. Growth Des*. **2006**, *6*, 2204-2206.
(52) Martínez-Lillo, J.; Armentano, D.; De Munno, G.; Marino, N.; Lloret, F.; Julve, M.; Faus, J. *CrystEngComm* **2008**, *10*, 1284-1287.
(53) Suzuki, K. I.; Kodama, T.; Kikuchi, K.; Fujita, W. *Chem. Lett*. **2010**, *39*, 1096-1098.
(54) Martínez-Lillo, J.; Armentano, D.; Mastropietro, T. F.; Julve, M.; Faus, J.; De Munno, G. *Cryst. Growth Des*. **2011**, *11*, 1733-1741.
(55) Armentano, D.; Martínez-Lillo, J. *Inorg. Chim. Acta* **2012**, *380*, 118-124.
(56) Martínez-Lillo, J.; Kong, J.; Julve, M.; Brechin, E. K. *Cryst. Growth Des*. **2014**, *14*, 5985-5990.
(57) Martínez-Lillo, J.; Pedersen, A. H.; Faus, J.; Julve, M.; Brechin, E. K. *Cryst. Growth Des*. **2015**, *15*, 2598-2601.
(58) Martínez-Lillo, J.; Cano, J.; Wernsdorfer, W.; Brechin, E. K. *Chem. - Eur. J*. **2015**, *21*, 8790–8798.
(59) Armentano, D.; Martínez-Lillo, J. *Cryst. Growth Des*. **2016**, *16*, 1812–1816.
(60) Adman, E.; Margulis, T. N. *Inorg. Chem*. **1967**, *6*, 210-214.
(61) Bouacida, S.; Merazig, H.; Beghidja, A.; Beghidja, Ch. *Acta Cryst*. **2005**, *E61*, m1153–m1155.
(62) Kahn, O. *Molecular Magnetism*; VCH: New York, 1993.
(63) Kleinberg, J. *Inorg. Synth*. McGraw-Hill, 1963.
(64) Earnshaw, A. Introduction to Magnetochemistry, Academic Press, London, Kahn, 1968.
(65) Bain, G. A.; Berry, J. F. *J. Chem. Educ*. **2008**, *85*, 532-536.
(66) Sheldrick, G. M. *Acta Cryst*. **2008**, *A64*, 112.
(67) Sheldrick, G. M. *Acta Cryst*. **2015**, *C71*, 3-8.
(68) SHELXTL; Bruker Analytical X-ray Instruments: Madison, WI, 1998.
(69) Palmer, D. CRYSTAL MAKER, Cambridge University Technical Services, C. No Title, 1996.

Enhancement of the Intermolecular Magnetic Exchange through Halogen···Halogen interactions in Bisadeninium Rhenium(IV) Salts

Donatella Armentano,[a] Miguel A. Barquero,[b] Carlos Rojas-Dotti,[b] Nicolas Moliner,[b] Giovanni De Munno,[a] Euan K. Brechin*[c] and José Martínez-Lillo*[b]

[a]Dipartimento di Chimica e Tecnologie Chimiche (CTC), Università della Calabria, via P. Bucci 14/c, 87036, Rende, Cosenza, Italy
[b]Instituto de Ciencia Molecular (ICMol), Universitat de València, c/ Catedrático José Beltrán 2, 46980, Paterna, Valencia, Spain
[c]EaStCHEM School of Chemistry, The University of Edinburgh, David Brewster Road, EH9 3FJ, Edinburgh, UK

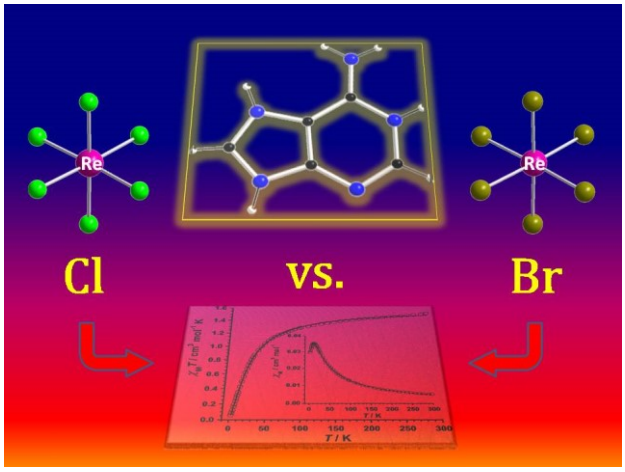

Two novel adenine-based Re^{IV} compounds have been synthesized and magneto-structurally characterized. Both compounds are isostructural hexahalorhenate(IV) salts that crystallize in the orthorhombic system with space group *Fdd*2. In the present work, we show how the substitution of coordinated chloride anions from the Re^{IV} complex by bromide ligands causes a significant enhancement of the intermolecular magnetic exchange between the paramagnetic metal ions.